SATELLITE MEASUREMENTS OF THE MOON'S MAGNETIC FIELD: A PRELIMINARY REPORT*

PAUL J. COLEMAN, JR.
Dept. of Planetary and Space Science, and Inst. of Geophysics and Planetary Physics, University of California, Los Angeles, Calif., U.S.A.

G. SCHUBERT
Dept. of Planetary and Space Science, University of California, Los Angeles, Calif., U.S.A.

C. T. RUSSELL
Inst. of Geophysics and Planetary Physics, University of California, Los Angeles, Calif., U.S.A.

and

L. R. SHARP
Dept. of Planetary and Space Science, and Inst. of Geophysics and Planetary Physics, University of California, Los Angeles, Calif., U.S.A.

Abstract. A preliminary analysis of the data from the UCLA magnetometer on board the Apollo 15 subsatellite indicates that remnant magnetization is a characteristic property of the Moon, that its distribution is such as to produce a rather complex pattern or fine structure, and that a detailed mapping of its distribution is feasible with the present experiment. The analysis also shows that lunar induction fields produced by transients in the interplanetary magnetic field are detectable at the satellite orbit so that in principle the magnetometer data can be used to determine the latitudinal and longitudinal as well as radial dependences of the distribution of electrical conductivity within the Moon. Finally, the analysis indicates that the plasma void or diamagnetic cavity which forms behind the Moon when the Moon is in the solar wind, is detectable at the satellite's orbit and that the flow of the solar wind near the limbs is usually rather strongly disturbed.

1. Introduction

Magnetic field measurements obtained with the Apollo 12 lunar surface magnetometer and the Apollo 14 hand-held magnetometer have established the existence of a significant lunar remnant magnetization, provided estimates of the distribution of electrical conductivity of the Moon's interior, and established an upper limit on the average magnetic permeability of the Moon. The objectives of the lunar subsatellite magnetometer experiment are to extend the measurements of the Moon's magnetic field, the permanent as well as the induced components, and to study the Moon's interaction with the fields and charged particles of its environment. Specific objectives include the following: to map the remnant magnetic field of the Moon, to map the electrical conductivity of the Moon's interior, and to study the properties of the plasmas in cis-lunar space by measuring the magnetic effects of the interactions of these plasmas with the Moon. Included in this objective is a search for magnetic disturbances caused by material that leaves the Moon by one process or another and is ionized while still nearby. Finally, the magnetometer is part of the instrumentation

* Publication No. 981. Institute of Geophysics and Planetary Physics.

Communication presented at the Conference on Lunar Geophysics, held between October 18–21, 1971, at the Lunar Science Institute in Houston, Texas, U.S.A.

for the lunar particle shadowing experiment. This experiment and its objectives are described in the Apollo 15 Preliminary Science Report.

The multiplicity of the objectives of the magnetic field study is made possible by the geometry of the Moon's orbit which, as shown in Figure 1, passes through three very different regions in near-Earth space, i.e., the region in which the solar wind flow is essentially undisturbed by the presence of the Earth, the 'magnetosheath' in which

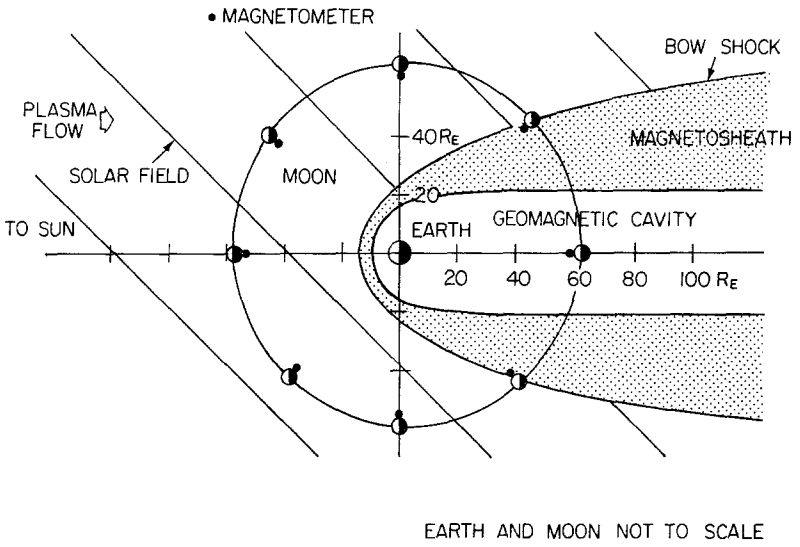

Fig. 1. Schematic diagram showing the three regions of near-Earth space traversed by the Moon. For most of each lunation the Moon is in the solar wind. The other two regions are the magnetosheath and the tail of the geomagnetic cavity. The plane of the figure is essentially the ecliptic plane. The large dot adjacent to the lunar surface marks the approximate location of the Apollo 12 lunar surface magnetometer.

the flow is drastically modified by the obstacle presented by the Earth's magnetic field, and the geomagnetic cavity which consists of the space threaded by the magnetic field from the Earth. As shown in the figure, this cavity extends to about 10 R_E in the direction of the Sun. Its extent in the opposite direction, i.e., the length of the geomagnetic tail, is unknown, although it is more than 70 R_E.

The lunar orbiting satellite, Explorer 35, has already yielded a great deal of information on the electromagnetic properties of the Moon and its interactions with its plasma environment. Orbits of this satellite for times separated by 6 months are shown in Figure 2. The area traversed by Explorer 35 during a 12-month period is indicated by bounding circles marking the loci of its periselenium and aposelenium. Also shown is the orbit of the subsatellite.

When the Moon is in the solar wind, the region directly behind the Moon, i.e., the region directly downstream from the Moon, is essentially devoid of solar wind plasma. This downstream cavity and the rarefaction waves on its boundary, shown schema-

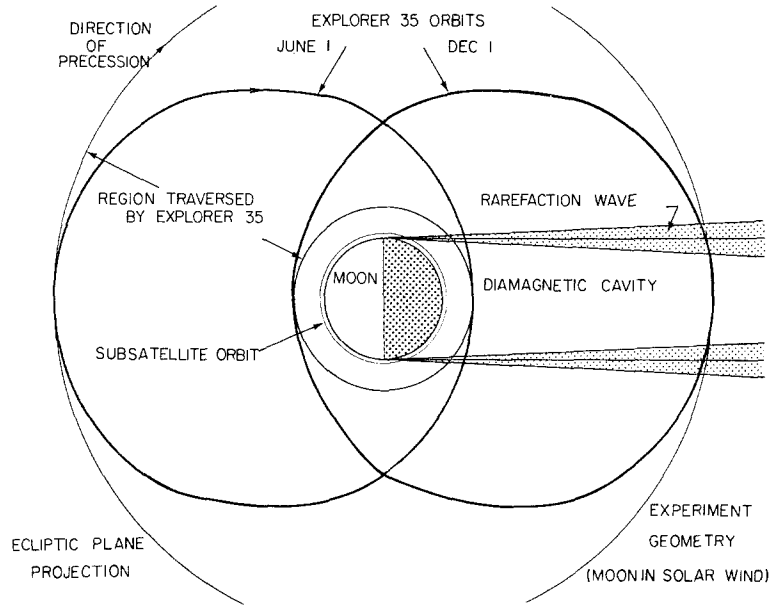

Fig. 2. Schematic diagram showing the interaction of the solar wind with the Moon. Also shown are the orbits of the lunar subsatellite and Explorer 35. The sketch is drawn as though the orbital planes of both are parallel to the ecliptic plane. Actually, the former is inclined to the ecliptic by about 25–30° while the latter is inclined by about 15°. Orbits of Explorer 35 are shown for times separated by 6 months. The region swept out by the Explorer 35 orbit over a 12-month interval is indicated by bounding circles.

tically in Figure 2, were discovered by Colburn *et al.* (1967) and Lyon *et al.* (1967) with instruments aboard Explorer 35. The sketches in Figures 1 and 2 show the essential difference between the interaction of the solar wind with the Moon and that with the Earth. Specifically, most of the solar wind that interacts with the Moon simply hits the Moon and stops (Figure 2), whereas most of the solar wind that interacts with the Earth is diverted around the entire geomagnetic cavity and forms the magnetosheath (Figure 1).

2. The Magnetometer

The magnetometer system carried on board the Apollo 15 subsatellite consists of two orthogonal fluxgate sensors mounted at the end of a 6-ft boom and an electronics unit housed in the spacecraft. A block diagram of the instrument is shown in Figure 3 and a photograph of the magnetometer hardware is shown in Figure 4. The specifications of the instrument are listed in Table I.

The two magnetometer sensors are oriented parallel (B_P) and transverse (B_T) to the spin axis of the spacecraft. The measured quantities used to define the vector field are the magnitude of the parallel component, the absolute value of the transverse component, and the angle between the transverse component and the component of the Sun-spacecraft vector transverse to the spin axis.

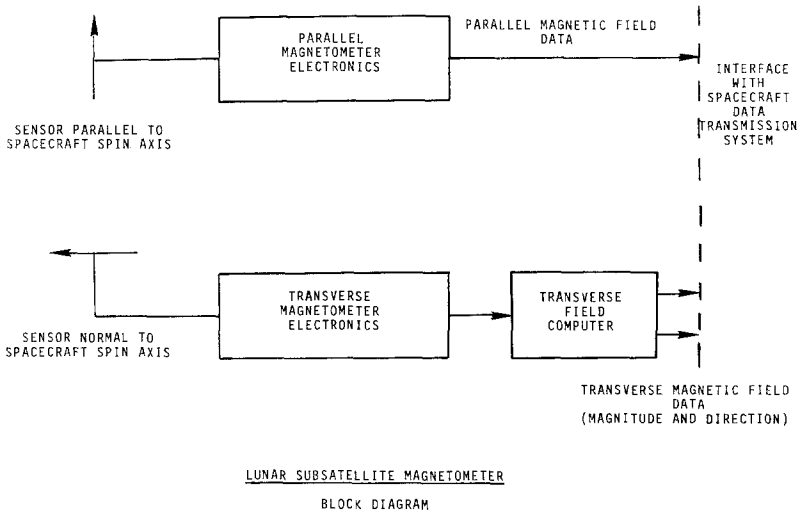

Fig. 3. Block diagram of the Apollo 15 subsatellite magnetometer.

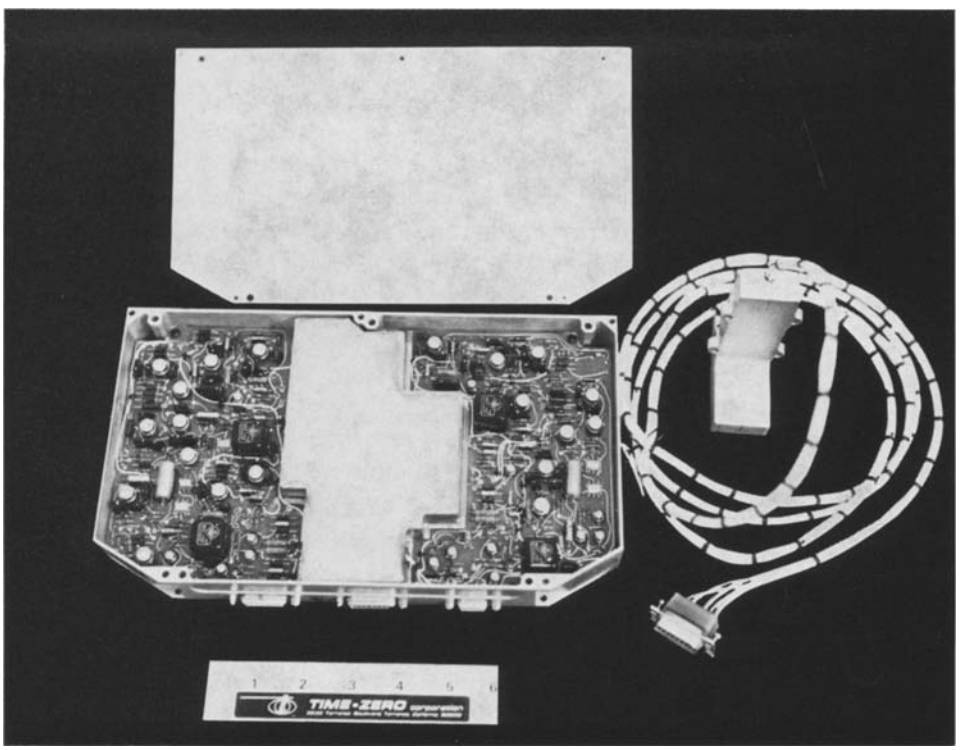

Fig. 4. Apollo subsatellite magnetometer.

TABLE I

Apollo subsatellite magnetometer specifications

Type:	Second-harmonic, saturable core fluxgate.
Sensor Configuration:	Two sensors, one sensor parallel to the satellite spin axis (B_P) and one perpendicular to this axis.
Mounting:	Sensor unit at end of 6-ft boom. Electronics unit in spacecraft body.
Dynamic Range:	Two ranges, automatically selected. 0-$\pm$50 γ at higher sensitivity. 0-$\pm$200 γ at lower sensitivity.
Resolution:	0.4 γ and 1.6 γ depending on range.
Sampling Rates:	
Real Time:	B_P every 2 s, B_T every s.
High Rate Storage:	B_P, B_T magnitude and B_T phase once every 12 s.
Low Rate Storage:	B_P, B_T magnitude and B_T phase once every 24 s.
Power:	0.70 W.
Weight:	Electronics Unit: 1.8 lb. Sensor Unit: 0.5 lb.
Size:	Electronics Unit: 11″ × 6.25″ × 1.5″ Sensor Unit: 0.6″ diam. × 3″.
Operating Temperature Range:	+160°F to −60°F.

An important item of subsatellite equipment is the data storage unit. This unit records field measurements on the far side of the Moon for playback when the subsatellite is in view from the Earth.

3. Remnant Magnetization

At times of relatively low levels of geomagnetic activity, the magnetic field in the geomagnetic tail is quite constant. Thus, the best possibilities for the detection of lunar remnant magnetism are provided by the subsatellite magnetometer data recorded when the Moon is in the geomagnetic tail during quiet intervals. Our preliminary analysis of the quick-look data recorded during the first two traversals of the geomagnetic tail revealed the existence of measurable levels of remnant magnetism over much of the subsatellite orbit. Figure 5 shows average values of B_P and B_T computed for 17 orbits during which the Moon was in the geomagnetic tail.

The major features of the structure in the traces, particularly in that of B_T, appear to be associated with large craters lying within 10° of the band defined by the ground tracks of the 17 orbits. We have numbered the seven most obvious local minima in B_T and named four of them with the associated craters. The most obvious feature is that apparently associated with the crater Van de Graaff, which produces a 1 γ variation in the field as the satellite sweeps past it. Van de Graaff is approximately 9° across and its center is located about 8° from the satellite ground track. Other prominent features of the data are associated with the craters Hertzsprung, Korolev, and Milne. The location of the average satellite ground track is shown in Figure 6. The numbered points along the track correspond to the numbered points in Figure 5.

The less obvious minimum at Point 4 may be associated with the crater Thomson in the sea of Ingenuity, south of the ground track, with the sea itself, or with the small crater Paracelsus lying directly underneath the track. The minimum at Point 5 may be associated with the crater Pavlov although the dip occurs somewhat beyond the crater position. Another possibility is that this point is just mid-way between radially

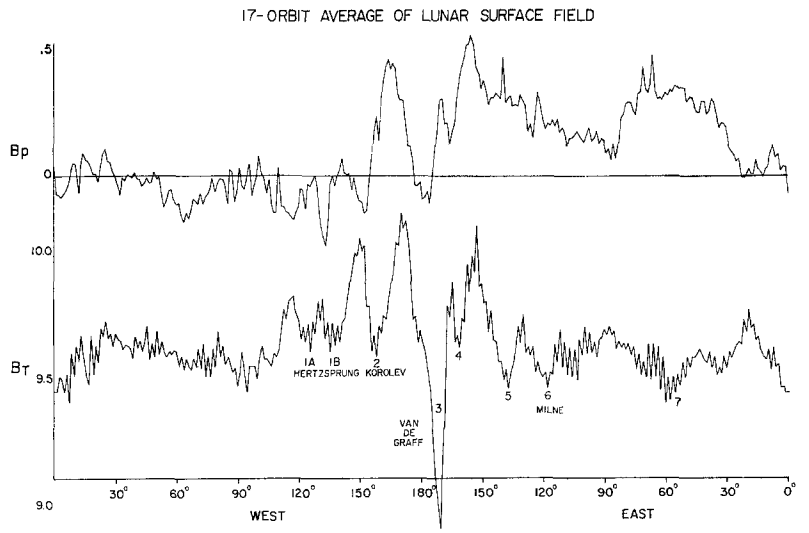

Fig. 5. Measurements of B_P and B_T obtained while the Moon was in the geomagnetic tail. The values plotted are averages over nine successive orbits. The longitudes of the intersections of perpendiculars from the centers and rims of nearby major craters with the satellite ground track are also shown. The measured values were derived from telemetered data using a preliminary calibration. Consequently, the absolute values may be in error by a few gammas although the indicated variations are accurate. The saw-tooth nature of the plots in certain regions is the result of statistical noise and the high resolution used for this plot.

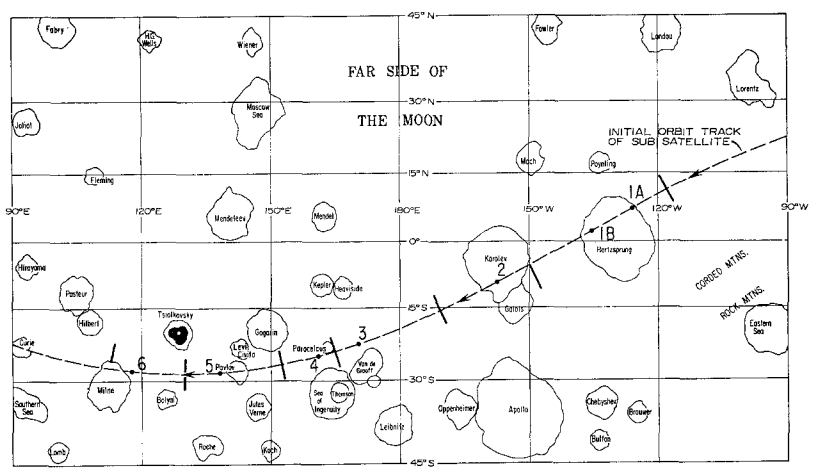

Fig. 6. Mercator projection of the far side of the Moon showing the ground track of the satellite for the fifth orbit in the nine orbit sequence used in Figure 5.

positive anomalies located on either side. If this is the case, the peaks would correspond to two craters lying to the north of the track, Gagarin and Tsiolkovsky.

The minimum at Point 7 occurs on the front side of the Moon and is possibly associated with the crater Langrenus.

The identification of the craters associated with each of these anomalies should be viewed with some caution. Since the process of averaging over 17 revolutions effectively filters out variations over latitude and longitude ranges of about 5° as well as temporal variations in the background field of the Earth's magnetotail, we have chosen to identify features with the largest nearby craters. However, some of these features may be associated with smaller craters.

The magnetic field measurements used in this preliminary analysis do not include the final pre-flight calibrations. Thus, although the measured variations are accurate, the absolute values of B_P are not necessarily correct. Further, the data processing performed to date has been done entirely by hand and this precluded our determining the orientation of the component perpendicular to the satellite spin axis. However, the preliminary results show that we will be able to obtain a detailed mapping of the lunar remnant magnetization from the subsatellite orbit.

The plot of B_T in the 17 orbit average shown in Figure 5 suggests that the remnant field is smoother and possibly weaker on the near side than on the far side and that most of the major craters produce local minima in B_T. Near side/far side asymmetry leads us to the speculation that the remnant field observed is due to irregularities in a magnetized crust. The crust has been disturbed over a broad region of the near side, possibly by the processes that created the ringed maria, but disturbed primarily by the formation of more localized craters on the far side.

Samples returned from the Apollo 11 and 12 sites show remnant magnetization as great as 10^{-2} emu/cm^3 (Runcorn *et al.*, 1970; Strangway *et al.*, 1970). If one takes this value as an upper limit on the magnetization of lunar material, then the minimum scale size of a spherical body magnetized at this level and producing a 1 γ variation at the subsatellite orbit is approximately 10 km. The field at the surface of such a region, and therefore the maximum field that could be produced by such a region on the surface of the Moon, is roughly 1000 γ. Such a volume would have a magnetic dipole moment of approximately 10^{16} G cm^3. For a more typical remnant magnetization of 10^{-5} emu/cm^3, the scale size would be 100 km and the surface field would be about 10 γ for this dipole moment. The data shown in Figure 5 also indicate that any lunar centered magnetic dipole must have a magnetic moment less than 4×10^{19} G cm^3 corresponding to a surface field strength in the range 1.5 to 3 γ.

A permanent magnetic field of 38 ± 3 γ was detected at the Apollo 12 site with the lunar surface magnetometer (Dyal *et al.*, 1970). Permanent fields of 103 ± 5 γ and 43 ± 6 γ were detected at sites separated by 1.12 km in the Fra Mauro region explored by the Apollo 14 astronauts (Dyal *et al.*, 1971). The lunar subsatellite has passed directly over both these sites, but no significant field variation was observed over either. Thus, the surface fields observed to date must be of relatively small scale size as indicated by the field gradient measured at the Apollo 14 site.

As the altitude of perilune of the subsatellite decreases, we will obtain more information on the fossil fields at the Apollo 12 and 14 sites. As pointed out by Sonett *et al.* (1971), if both were produced by the same magnetizing field, a field in excess of $10^3\ \gamma$ must have existed some billion years after the formation of the Moon, or 3.4 billion years ago, and further, it must have existed for 300 million years, since the magnetized rocks from the Apollo 11 and 12 sites are respectively 3.4 and 3.7 billion years old. A detailed map of the permanent magnetization on the Moon will provide additional information on the ancient magnetizing field, and the history of the magnetized material subsequent to its magnetization.

4. Electrical Conductivity

Information on the electrical conductivity of the Moon's interior has been obtained through an analysis of simultaneous magnetic field measurements at the Apollo 12 site and at the lunar orbiting satellite, Explorer 35. The results already obtained include a radial conductivity profile that has been interpreted in terms of models of mantle-core stratification, the mantle temperature, the near-surface thermal gradient and heat flux, and the composition of the interior (Dyal and Parkin, 1971; Sonett *et*

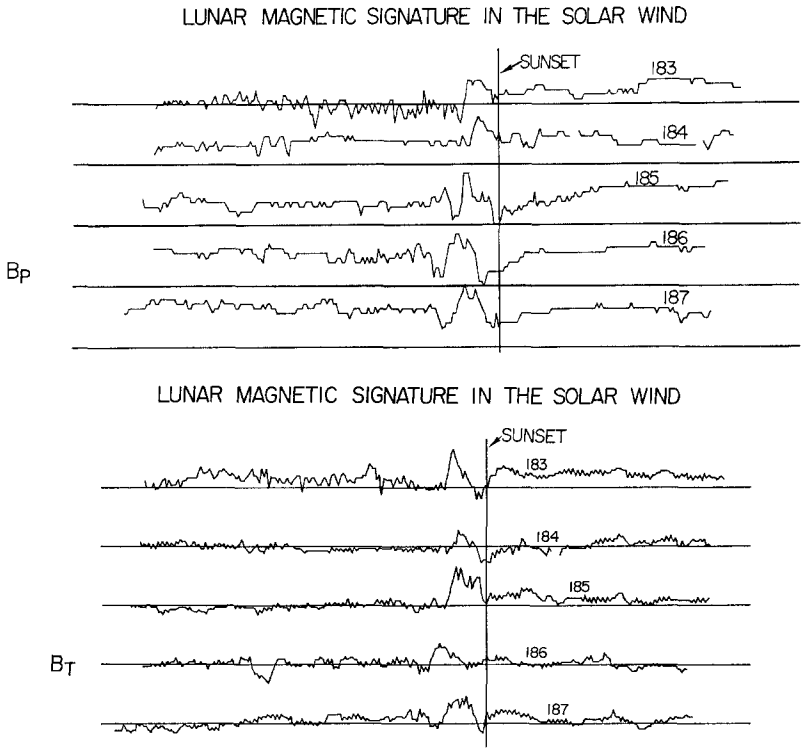

Fig. 7a–b. Plots of B_P and B_T for five consecutive orbits during which the Moon was in the solar wind.

al., 1971a,b). The experimental method employed in these studies is essentially a measurement of the Moon's response to changes in the solar wind magnetic field.

Data recorded at the lunar subsatellite during several successive orbits when the Moon was in the solar wind are plotted in Figure 7. From the point of view of the conductivity studies, the important feature of these plots is the greater variability of the magnetic field on the day side or upstream side of the Moon. This behavior suggests that the magnetic field measured at the subsatellite when the Moon is in the solar wind includes a component due to lunar induction. The presence of this component indicates that data from the subsatellite magnetometer, along with simultaneous data from the lunar surface magnetometers and Explorer 35 magnetometer, can be used to produce a detailed, three-dimensional model of the interior conductivity. At this writing, the conductivity studies are only just beginning and no further results are available.

5. Boundary Layer Studies

Observations of the magnetic field and plasma obtained with the lunar orbiter, Explorer 35, have revealed a fairly consistent picture of the large-scale interaction of the solar wind with the Moon. As shown schematically in Figure 2, the absence of a lunar bow shock allows most of the solar wind plasma to reach the lunar surface where it is absorbed. As a consequence of this absorption, a so-called diamagnetic cavity exists behind the Moon, or downstream from the Moon, when the Moon is in the solar wind. The essential magnetic feature of this cavity is an interior magnetic

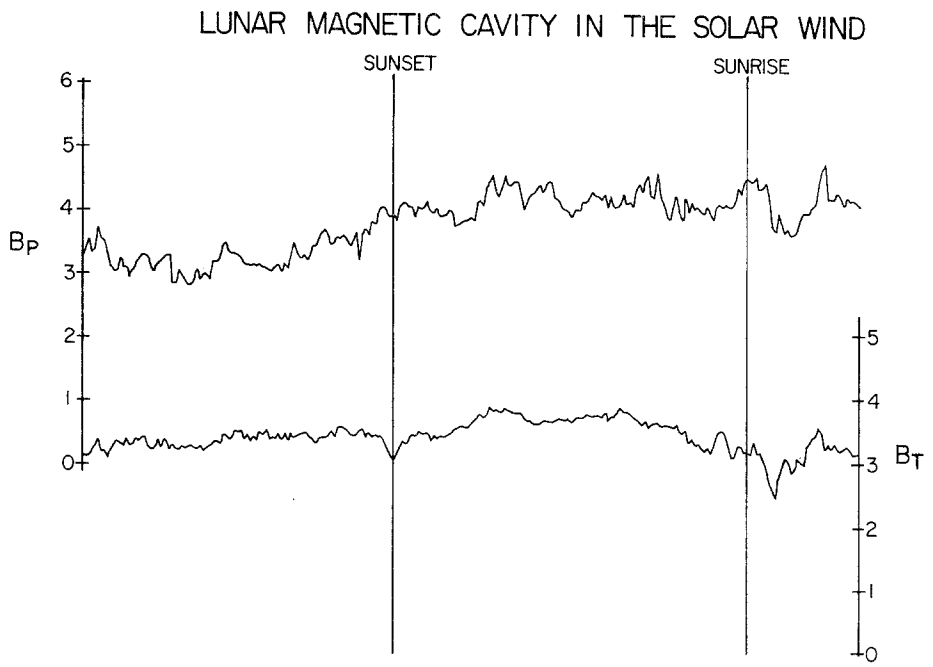

Fig. 8. Averages of B_P and B_T computed from 12 orbits during which the Moon was in the solar wind.

field stronger by about 1.5 γ, on the average, than the exterior field. At the boundary of this cavity, there is a sharply localized decrease in the field magnitude approximately coincident with the boundary of the Moon's optical shadow (Colburn *et al.*, 1967).

The preliminary analysis of the data from the subsatellite magnetometer indicates that a diamagnetic increase also appears at the lower altitude of the subsatellite. Figure 8 shows a 12-orbit average of the measurements recorded while the Moon was in the solar wind. The field enhancement between satellite sunset and satellite sunrise is readily distinguishable and is approximately 1 γ.

Data from Explorer 35 have also revealed the existence of sporadic field disturbances adjacent to the rarefaction wave at the boundary of the diamagnetic cavity (see Figure 2). Mihalov *et al.* (1971) have shown that these disturbances occur in the solar wind flow across the limbs when certain regions of the lunar surface are at the limbs. The greatest concentration of disturbance sources was found to be in a 15° square near the crater Gagarin.

Our preliminary analysis of the subsatellite magnetometer data indicates that strong disturbances, or limb effects, are present most of the time. These disturbances produce more or less characteristic variations in the subsatellite magnetometer record. Record sections from orbits 183–187 are shown in Figure 7. The data analyzed so far suggest that the disturbances, such as those apparent near the sunset line, occur when near-side regions are at the limbs as well as when far-side regions are there. A 12 orbit average plotted in Figure 8 shows that limb effects at satellite sunrise, i.e., at the sunset limb on the Moon, are more persistent than those at the other limb. It remains to be seen whether this persistence is a consequence of this area's being more effective in producing disturbances or some property of the solar wind, such as the orientation of its magnetic field. Thus, on the one hand the detection of relatively strong remnant fields in the vicinity of Gagarin is consistent with the suggestion of Mihalov *et al.* that the limb effects detected at Explorer 35 are caused by localized regions of enhanced magnetic fields. On the other hand, the preliminary indication from the subsatellite data that limb disturbances are present more often than not and that they are just as great when many other regions are at the limb indicates that further study is required to establish the causes of these disturbances in the solar wind across the limbs.

6. Summary

Our preliminary analysis of the data from the UCLA magnetometer on board the Apollo 15 subsatellite indicates that remnant magnetization is a characteristic property of the Moon, that its distribution is such as to produce a rather complex pattern or fine structure, and that a detailed mapping of its distribution is feasible with the present experiment. More specifically, the data taken during the first pass through the geomagnetic tail indicate that the craters, at least those with diameters of over 100 km and greater, have qualitatively similar magnetic signatures. The analysis also shows that lunar induction fields produced by transients in the interplanetary magnetic field are detectable at the satellite orbit and that the magnetometer data will provide

estimates of the latitude and longitude dependences in the distribution of interior conductivity. Finally, the analysis indicates that the plasma void or diamagnetic cavity that forms behind the Moon when the Moon is in the solar wind is detectable at the satellite's orbit and that the flow of the solar wind across the limbs is usually rather strongly disturbed. However, the specific characteristics of the field produced by this disturbed flow appear to depend partly on the surface regions at the limbs.

It should be emphasized that these conclusions are, for the most part, tentative. Their verification must await more detailed analysis, improvements in statistical accuracy, and comparisons with the lunar surface magnetometers and the Explorer 35 magnetometer.

Acknowledgments

We are indebted to G. Takahashi and his staff at Time Zero, Inc., for their efforts in the design and fabrication of the subsatellite magnetometer; and to T. Pederson, R. Brown, and their staff at TRW Systems, Inc., for their work in the design, fabrication and testing of the subsatellite and the integration of the magnetometer. We are particularly grateful to C. Thorpe who was charged with the difficult task of controlling the magnetic fields of the subsatellite.

The UCLA engineering team was led by R.C. Snare. Preliminary circuit designs were done by the late R.F. Klein. The testing and calibration of the magnetometer was supervised by F.R. George.

We are also grateful to the many people at the Manned Spacecraft Center who contributed to the success of this project, especially J. Johnson, the program manager, and P. Lafferty, the technical monitor for our project.

No list of acknowledgments for this experiment can be complete without an expression of appreciation to astronauts Scott, Irwin, and Worden. Through their efforts Apollo 15 opened a new era of space exploration.

References

Colburn, D. S., Currie, R. G., Mihalov, J. D., and Sonett, C. P.: 1967, *Science* **158**, 1040.

Dyal, P., Parkin, C. W., and Sonett, C. P.: 1970, *Science* **196**, 762.

Dyal, P. and Parkin, C. W.: 1971, 'The Apollo 12 Magnetometer Experiment: Internal Lunar Properties from Transient and Steady Magnetic Field Measurements', *Proceedings Second Lunar Science Conference* **3**, 2391–2413.

Dyal, P., Parkin, C. W., Sonett, C. P., DuBois, R. L., and Simmons, G.: 1971, 'Lunar Portable Magnetometer Experiment', Preprint, NASA-Ames Research Center.

Lyon, E. F., Bridge, H. S., and Binsack, J. H.: 1967, *J. Geophys. Res.* **72**, 6113.

Mihalov, J. D., Sonett, C. P., Binsack, J. H., and Moutsoulas, M. D.: 1971, *Science* **171**, 892.

Runcorn, S. K., Collinson, D. W., O'Reilly, W., Battey, M. H., Stephenson, A. A., Jones, J. M., Manson, A. J., and Readman, P. W.: 1970, *Geochim. Cosmochim. Acta., Suppl.* 1, **3**, 2369.

Sonett, C. P., Colburn, D S., Dyal, P., Parkin, C. W., Smith, B. F., Schubert, G., and Schwartz, K.: 1971a, *Nature* **230**, 359.

Sonett, C. P., Schubert, G., Smith, B. F., Schwartz, K., and Colburn, D. S.: 1971b, 'Lunar Electrical Conductivity from Apollo 12 Magnetometer Measurements: Compositional and Thermal Inferences', *Proceedings, Second Lunar Science Conference* **3**, 2415–2431.

Strangway, D. W., Larson, E. E., and Pearce, C. W.: 1970, *Geochim. Cosmochim., Acta., Suppl.* 1, **3**, 2534.